Simultaneous Excitatory and Inhibitory Dynamics in A Graphene Excitable Laser

Philip Y. Ma*, Bhavin J. Shastri*, Alexander N. Tait, Mitchell A. Nahmias, Thomas Ferreira de Lima, and Paul R. Prucnal

Department of Electrical Engineering, Princeton University, Princeton, NJ 08544, USA
**These authors contributed equally to this work.*
yechim@princeton.edu

Abstract: We demonstrate experimentally for the first time the simultaneous excitatory and inhibitory dynamics in a graphene excitable laser. This technology potentially opens novel spike processing functionality for future neuromorphic photonic systems.

OCIS codes: (070.4340) Nonlinear optical signal processing; (200.4700) Optical neural systems.

Photonic neuromorphic spike processing has emerged in recent years as a promising candidate of unifying the communication and computation on the same platform [1–3]. Spiking is a hybrid information processing technique combining both the bandwidth efficiency of analog processing and noise robustness of digital computation [4]. Due to its strong analogy with the biological neuron in terms of their underlying excitability mechanisms [5], neuromorphic photonic system grants huge capacity for complex, ultrafast categorization and decision-making [6]. Lasers operating in the excitable regime (i.e., excitable lasers) used in conjunction with saturable absorber (SA), in particular, have exhibited novel spike processing features such as sharp thresholding and temporal integration [1, 7].

The role of inhibition in neural circuit function is well established to be essential in all but special cases [8, 9]. In photonic signal processing, the use of power envelopes to represent signals raises challenges in effecting inhibitory and excitatory responses. This functionality might be achieved in the linear network portion using balanced photodetectors [10], which necessitates optical-to-electrical conversion. Ref. [11] showed the use of multiple wavelengths to effect opposing perturbations; but, lacking excitability dynamics, this device did not produce sharp all-or-none responses [7]. Another approach used optical phase to control the effective sign of a perturbation on an excitable laser [12]; however, coordinating the relative optical phases of a network of independent lasers presents a theoretical challenge.

Here, we report experimentally for the first time the excitability mechanism of a graphene excitable laser in response to both the excitatory and inhibitory inputs. Our approach employs a graphene excitable fiber laser for a proof-of-principle demonstration. We measure the spike output energy versus the timing difference between the excitatory and inhibitory inputs, and discover (1) almost zero spike output when the the excitatory input coincides temporally with the inhibitory input, (2) strong spike output suppression if the inhibitory input is temporally close to but ahead of the excitatory input, (3) close correlation between the inhibition recovery time and spike output duration as a result of a single excitatory input.

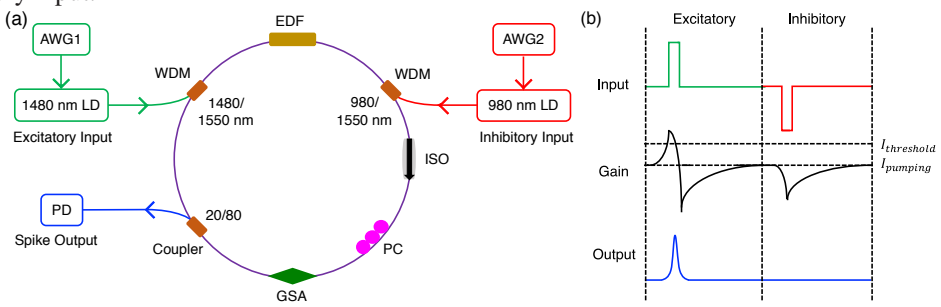

Fig. 1: (a) Experimental setup of the graphene excitable fiber laser in subject to both the excitatory and inhibitory inputs. (b) Schematic illustration of the excitable laser dynamics in response to the excitatory and inhibitory inputs, respectively.

Fig. 1(a) shows the experimental setup of the graphene excitable fiber laser. The whole fiber ring cavity consists of a 75-cm long gain medium of highly-doped erbium-doped fiber (EDF) and a chemically synthesized graphene saturable absorber (GSA) sandwiched between two fiber connectors. The gain and SA sections are separated by an isolator (ISO) to ensure unidirectional propagation and a polarization controller (PC) to enhance output pulse stability. Two arbitrary waveform generators (AWG1 and AWG2) are used to produce excitatory and inhibitory patterns, respectively. AWG1 modulates a 1480 nm laser diode (LD) to generate the excitatory input while AWG2 modulates a 980 nm LD to generate the inhibitory input. A 1480/1550 nm wavelength division multiplexer (WDM) and a 980/1550 nm WDM are used to guide the excitatory and inhibitory inputs to the EDF. The spike output is decoupled out of the system through

the 20/80 coupler to a photodiode (PD). Fig. 1(b) illustrates the excitable laser dynamics with individual excitatory and inhibitory inputs. On one hand, the high level of the inhibitory input is set to the pumping level ($I_{pumping}$) where the excitatory input can build up the gain level above the excitability threshold ($I_{threshold}$), and saturate the GSA to transparency to releases a spike output. On the other hand, the low level of the inhibitory input lowers the gain level, which increases the amount of the excitatory input that will be required to reach the excitability threshold.

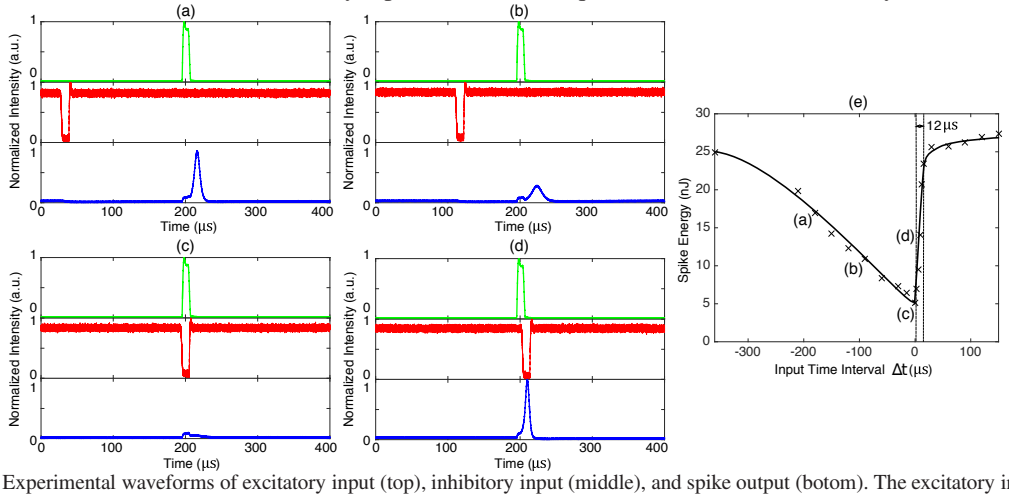

Fig. 2: (a)-(d) Experimental waveforms of excitatory input (top), inhibitory input (middle), and spike output (botom). The excitatory input is leading the inhibitory input by (a) -180 μs, (b) -90 μs, (c) 0 μs, and (d) 9 μs. (e) Spike output energy versus input time interval Δt which measures the time by which the excitatory input is leading the inhibitory input.

Fig. 2 shows experimental results of using the graphene excitable laser to process the coexisting excitatory and inhibitory inputs. It can be seen that the spike output is greatly suppressed as the inhibitory input gradually reduces the time period by which it is leading the excitatory input (Fig. 2(a)-(b)). Nearly complete spike output suppression occurs when these two inputs overlap in time (Fig. 2(c)). However, the spike output experiences a quick recovery as soon as the inhibitory input is lagging the excitatory input (Fig. 2(d)). These results corroborate circuit model simulations of two-section gain-SA lasers performed in [13], and are explicitly shown in Fig. 2(e) where we measure the spike output energy versus the input time interval. The strong slope contrast between the falling and rising edges indicates that the spike output suppression quickly decays as the inhibitory input is temporally lagging the excitatory input. The reason can be attributed to Fig. 1(b) where the inhibitory input initiates a long-lasting gain depression effect only from the moment it is introduced. The inhibition recovery time, i.e., 10% to 90% rising time of the rising edge, is measured to be 12.0 μs. This is close to the spike output duration under no inhibitory input, which is measured to be 11.6 μs in our experiment. Such a close correlation makes sense by considering that the inhibitory input should have negligible effect on the spike output if it lags the excitatory input by the time it takes the spike energy to be released.

In conclusion, we present the first experimental demonstration of simultaneous excitatory and inhibitory dynamics in a graphene excitable laser. We observe a strong spike output suppression effect when the inhibitory input can be temporally close to but ahead of the excitatory input. We also find close correlation between the inhibition recovery time and spike output duration as a result of a single excitatory input. Future work will involve studying the effect of noise (amplitude and timing jitter), demonstration of simple winner-takes-all circuits for unsupervised learning, and a theoretic approach to study the observed dynamics corroborated with detailed analysis. Ultimately, photonic spike processing could bring advanced neural network processing functions into ultrafast computing regimes.

References

1. F. Selmi, et. al., "Relative refractory period in an excitable semiconductor laser," Phys. Rev. Lett. **112**, 183902 (2014).
2. B. Romeira, et. al., "Regenerative memory in time-delayed neuromorphic photonic resonators, Scientific Reports **6**, 19510 EP – (2016).
3. P. R. Prucnal, et. al., "Recent progress in semiconductor excitable lasers for photonic spike processing," Advances in Optics and Photonics, **8**(2), 228–299 (2016).
4. R. Sarpeshkar, et. al., "Analog versus digital: extrapolating from electronics to neurobiology," Neural Comput. **10**(7), 1601–1638 (1998).
5. M. A. Nahmias, et. al., "A leaky integrate-and-fire laser neuron for ultrafast cognitive computing," IEEE J. Sel. Tops. Quantum Electron. **19**, 1800212 (2013).
6. A. N. Tait, et. al., "Photonic neuromorphic signal processing and computing," in Nanophotonic Information Physics, ser. Nano-Optics and Nanophotonics, M. Naruse, Ed. Springer Berlin Heidelberg, 2014, pp. 183–222.
7. B. J. Shastri, et. al., "Spike processing with a graphene excitable laser," Sci. Rep. **6**, 19126; doi:10.1038/srep19126 (2016).
8. S. Ostojic, et. al., "Two types of asynchronous activity in networks of excitatory and inhibitory spiking neurons," Nature neuroscience, **17** 594–600 (2014).
9. A. R. Aron, et. al., "The neural basis of inhibition in cognitive control," The Neuroscientist, **13**(3):214–228 (2007).
10. A. N. Tait, et. al., "Broadcast and weight: An integrated network for scalable photonic spike processing," J. Lightwave Technol., **32**(21):3427-3439 (2014).
11. K. Kravtsov, et. al., "Ultrafast all-optical implementation of a leaky integrate-and-fire neuron," Optics express, **19**, 2133–2147 (2011).
12. K. Alexander, et. al., "Excitability in optically injected microdisk lasers with phase controlled excitatory and inhibitory response," Optics express, **21**, 26182–26191 (2013).
13. B. J. Shastri, et. al., "SIMPEL: Circuit model for photonic spike processing laser neurons," Opt. Express **23**, 8029-8044 (2015).